Disrupted Resting-State Functional Connectivity in Nonmedicated Bipolar Disorder[1]

Ying Wang, PhD
Shuming Zhong, MD
Yanbin Jia, MD
Yao Sun, MD
Bing Wang, MD
Tao Liu, MD
Jiyang Pan, PhD
Li Huang, MD

Purpose: To investigate the whole-brain intrinsic functional connectivity patterns of patients with bipolar disorder (BD).

Materials and Methods: This prospective study was approved by the research ethics committee, and all participants provided informed consent. Thirty-seven patients with nonmedicated BD II depression and 37 healthy control participants underwent resting-state functional magnetic resonance (MR) imaging. Whole-brain connectivity was analyzed by using a graph theory approach: functional connectivity strength (FCS). Clinical state was assessed by using the 24-item Hamilton Depression Rating Scale and the Young Mania Rating Scale. Two-sample *t* test and nonparametric correlation analysis were used.

Results: Compared with healthy control participants, patients with BD II showed decreased FCS in the default mode network (ie, the bilateral medial prefrontal cortex, bilateral middle temporal gyrus, left precuneus, and right posterior cingulate cortex), right supramarginal gyrus and angular gyrus, right superior frontal gyrus, and right superior parietal gyrus and increased FCS in the bilateral temporal pole (including the parahippocampal gyrus and amygdale), left anterior cingulate cortex, left superior temporal gyrus, right lingual gyrus, and left anterior lobe of the cerebellum ($P < .05$; AlphaSim corrected).

Conclusion: These results suggest that patients with BD have disrupted intrinsic functional connectivity mainly in the default mode network and limbic system, which might be associated with the pathophysiologic structure of BD.

[1] From the Clinical Experimental Center (Y.W.), Medical Imaging Center (Y.W., Y.S., L.H.), and Department of Psychiatry (S.Z., Y.J., B.W., T.L.), First Affiliated Hospital of Jinan University, Guangzhou 510630, China. Received July 25, 2015; revision requested September 29; revision received November 18; accepted December 17; final version accepted December 28. **Address correspondence to** Y.W. (e-mail: *johneil@vip.sina.com*).

Supported by the National Science Foundation of China (81501456, 81471650); Natural Science Foundation of Guangdong Province, China (2014A030313375); Planned Science and Technology Project of Guangdong Province, China (2014B020212022); Research Funds for the Central Universities of China (21615476); Planned Science and Technology Project of Guangzhou, China (1563000653, 155700029). The funders had no role in the study design, data collection and analysis, decision to publish, or preparation of the manuscript.

Bipolar disorder (BD) is a chronic, severe, and fluctuating psychiatric disorder, and it is a leading cause of premature mortality from suicide and associated medical conditions, such as diabetes mellitus and cardiovascular and neurovascular disease. It is characterized by the core feature of recurrence of mania (BD I) or hypomania (BD II) and depressive episodes that seriously affect the quality of life and social functions of patients (1). Although a growing number of structural and functional neuroimaging studies revealed abnormalities in specific brain areas and connections in BD, the neurobiology of BD is incompletely understood.

Resting-state functional magnetic resonance (MR) imaging is a noninvasive neuroimaging technique that can measure spontaneous or intrinsic brain activity (2). Previous studies (3–7) suggested that there were widespread local functional abnormalities in multiple brain regions in BD, including the medial prefrontal cortex, anterior cingulate cortex, thalamus, pallidostriatum, amygdala, and hippocampus. Changes in functional connectivity were identified (5,8–12) between specific regions, such as default-mode network, thalami-striatum connectivity, anterior cingulate-amygdalae connectivity, and prefrontal-limbic connectivity, by using independent component analysis and seed-based correlation analysis. In recent years, graph theory metrics were applied to resting-state functional MR imaging datasets to derive measures of whole-brain functional connectivity. Several studies found altered topologic organization of large-scale functional brain networks in neuropsychiatric diseases, such as Alzheimer disease (13,14), posttraumatic stress disorder (15), schizophrenia (6,16), and major depressive disorder (17,18). For BD, there was only one electroencephalogram study that showed disrupted functional topological architecture of resting-state brain network in patients with BD I (19). In addition, the network architecture of functional connectivity within the human brain connectome is poorly understood at the voxel level (20).

In our study, we used resting-state functional MR imaging data and voxel-based graph theory analysis to investigate the whole-brain intrinsic functional connectivity patterns of patients with BD.

Advance in Knowledge

- In patients with bipolar disorder (BD), we observed decreased functional connectivity strength (FCS) values in the default mode network (ie, bilateral medial prefrontal cortex, bilateral middle temporal gyrus, left precuneus, and right posterior cingulate cortex), right supramarginal gyrus and angular gyrus, right superior frontal gyrus, and right superior parietal gyrus and increased FCS values in the bilateral temporal pole, left anterior cingulate cortex, left superior temporal gyrus, right lingual gyrus, and left cerebellum ($P < .05$; AlphaSim corrected).

Implication for Patient Care

- The brain regions of the default mode network and limbic system may be targets for development of future therapeutic interventions for BD.

Materials and Methods

Participants

This prospective study was approved by the Ethics Committee of First Affiliated Hospital of Jinan University (Guangzhou, China), and written informed consent for each participant was obtained before the study. Patients were recruited from May 2013 to March 2015. In total, 41 right-handed, out- or in-patients with BD II were recruited from the psychiatry department of our hospital (First Affiliated Hospital of Jinan University). The patients ranged in age from 18 to 55 years. All patients met Diagnostic and Statistical Manual of Mental Disorders, Fourth Edition (known as DSM-IV) criteria for BD II according to the diagnostic assessment by the Structured Clinical Interview for DSM-IV Patient Edition. Diagnosis of BD was determined by two experienced clinical psychiatrists (Y.J. and S.Z., with 20 and 5 years of experience in clinical psychiatry, respectively). Exclusion criteria included the presence of the following: *(a)* any current psychiatric disorder (with the exception of BD and anxiety disorders); *(b)* a history of electroconvulsive therapy; *(c)* any history of moderate or severe head injury, head trauma, neurologic disorder, or mental retardation; *(d)* alcohol or substance abuse or dependence; and *(e)* the presence of a concurrent and major physical illness. No patients were excluded because of the exclusion criteria. Clinical state was assessed by using the 24-item Hamilton Depression Rating Scale and the Young Mania Rating Scale during the 7-day period before the imaging session. All patients with BD were diagnosed with depression (Hamilton Depression Rating Scale score, ≥18). At the time of testing, all patients either had not been administered medication or were not medicated for at least 6 months. A total of 38 right-handed healthy control participants were recruited via local advertisements. They were carefully screened through a diagnostic interview, the Structured Clinical Interview for DSM-IV Nonpatient Edition, to rule out the

Published online before print
10.1148/radiol.2016151641 **Content code:** NR

Radiology 2016; 280:529–536

Abbreviations:
BD = bipolar disorder
FCS = functional connectivity strength

Author contributions:
Guarantors of integrity of entire study, Y.W., Y.J., J.P., L.H.; study concepts/study design or data acquisition or data analysis/interpretation, all authors; manuscript drafting or manuscript revision for important intellectual content, all authors; approval of final version of submitted manuscript, all authors; agrees to ensure any questions related to the work are appropriately resolved, all authors; literature research, Y.W., Y.J., L.H.; clinical studies, Y.W., Y.S., B.W., J.P., L.H.; experimental studies, Y.J., B.W.; statistical analysis, Y.W., B.W., J.P.; and manuscript editing, Y.W., L.H.

Conflicts of interest are listed at the end of this article.

presence of current or past psychiatric illness. Further exclusion criteria for healthy control participants were any history of psychiatric illness in first-degree relatives and current or past significant medical or neurologic illness. Data on 20 patients were published in a recent study (21) of our group that used resting-state functional MR imaging data and voxel-mirrored homotopic connectivity analysis, which quantified functional homotopy by providing a voxelwise measure of connectivity between hemispheres. This method measured functional connectivity between each voxel in one hemisphere and its mirrored counterpart in the opposite hemisphere, which is different from the current study of voxel-based graph theory analysis.

MR Imaging Data Acquisition and Preprocessing

MR imaging data were acquired on a 3-T MR system (Discovery MR 750 System; GE Healthcare, Milwaukee, Wis) with an eight-channel phased-array head coil. Functional images were acquired by using gradient-echo echo-planar imaging sequence with the following parameters: repetition time (msec)/echo time (msec), 2000/25; flip angle, 90°; 35 axial sections per volume; section thickness, 3 mm; intersection gap, 1 mm; 64 × 64 matrix; field of view, 240 × 240 mm^2; and voxel size, 3.75 × 3.75 × 3 mm^3. For each participant, 210 volumes were acquired, which resulted in an imaging time of 420 seconds. The participants were instructed to relax with their eyes closed without falling asleep. In addition, a three-dimensional brain volume imaging sequence that covered the whole brain was used for structural data acquisition (8.2/3.2; flip angle, 12°; 256 × 256 matrix; field of view, 240 × 240 mm^2; section thickness, 1 mm; no intersection gap). All MR images were evaluated by two neuroradiologists (Y.W. and Y.S., with 8 and 3 years of experience in neuroimaging, respectively).

Functional Image Preprocessing

Image preprocessing was performed by using Statistical Parametric Mapping (SPM8;*http://www.fil.ion.ucl.ac.uk/spm*) and Data Processing Assistant for Resting-State fMRI (22). For each participant, the first 10 images were discarded to ensure steady-state longitudinal magnetization. The remaining images were section-time corrected and realigned to the first image in the first series. All participants had no more than 2 mm of maximum displacement in x-, y-, or z-axis, and 2° of angular motion. The individual T1-weighted images were coregistered to functional images. The coregistered T1-weighted structural images were segmented (gray matter, white matter, and cerebrospinal fluid) by using the unified segmentation algorithm, and they were then transformed into standard Montreal Neurologic Institute space. The functional images were also spatially normalized to Montreal Neurologic Institute space by applying the parameters of structural image normalization and were resampled to 3 × 3 × 3 mm^3 resolution. Further preprocessing included linear trend removal and temporal band-pass filtering (0.01–0.08 Hz). Finally, the nuisance signals (six head motion parameters, global mean signal, cerebrospinal fluid signal, and white matter signal) were regressed out from the time course of each voxel. The residuals were used for resting-state functional connectivity analysis that followed.

Whole-Brain Functional Connectivity Analysis

Whole-brain resting-state functional connectivity analysis was performed by using the Gretna (*www.nitrc.org/projects/gretna/*) packages (23). First, we computed Pearson correlation coefficient between the time series of all pairs of gray matter voxels and obtained a whole-brain functional connectivity matrix for each individual. This computation was constrained within a gray matter mask that was generated by setting a threshold of 0.2 on the mean map of all gray matter maps involving all participants. Individual correlation matrices were transformed into a *z*-score matrix by using a Fisher *r*-to-*z* transformation to improve normality for group level *t* tests. Then, for a given voxel, functional connectivity strength (FCS) was computed as the sum of the connections (*z* values) between a given voxel and all other voxels. By considering the ambiguous interpretation of negative correlations with removal of the global signal, we conservatively restricted our analysis to positive correlations above a threshold of $r = 0.25$ (18,24,25). Such a threshold was chosen to eliminate the voxels with weak correlations that possibly arise from signal noise. To evaluate the effects of different correlation thresholds, we also analyzed FCS with different thresholds of *r* values of 0.2, 0.3, and 0.4, respectively (these results did not change our main conclusion; data not shown). Moreover, Buckner et al (24) indicated that different threshold selections did not qualitatively change the results. Notably, an FCS metric is similar to the so-called weighted degree centrality of networks in terms of graph theory (18,24,26). Finally, all individual FCS maps were further spatially smoothed (Gaussian smoothing kernel full-width at half maximum, 6 mm) (18,25). All the data were analyzed by two authors (Y.W. and Y.S., with 5 and 3 years of experience in MR research, respectively).

Statistical Analysis

Independent-sample *t* tests and χ^2 tests were used to compare the demographic data between the BD and healthy control groups with software (SPSS 17.0; SPSS, Chicago, Ill). The one-sample *t* test was performed to demonstrate the spatial distribution of FCS maps in BD and control participants. The two-sample *t* test was performed to determine the significant differences in FCS maps between patients with BD and control participants. The statistical threshold was set at corrected *P* value of less than .05 (combination of $P < .01$ for single voxel and a minimum cluster volume of >1161 mm^3), which was determined by Monte Carlo simulations by using the AlphaSim program (AFNI; *http://afni.nimh.nih.gov/pub/dist/doc/manual/AlphaSim.pdf*). Age, sex, and head motion parameters were included as nuisance covariates. When

statistically significant group differences were observed in any brain regions, we computed the Pearson correlation coefficients between FCS values and the clinical variables in patients with BD. These clinical variables included the Hamilton Depression Rating Scale scores, number of episodes, onset age of illness, and duration of illness. The threshold for significance was adjusted for multiple comparisons by using Bonferroni correction (27).

Results

Demographic Data and Clinical Comparisons

Table 1 shows the demographic and clinical data of all study participants. Four patients with BD and one control participant were excluded from further analyses because of excessive head motion during the image acquisition. Finally, the participants were 37 patients with BD II and 37 healthy control participants. There were no significant differences in sex, age, and years of education between the BD group and the healthy control group ($P > .05$).

Table 1

Demographic and Clinical Data in Patients with BD and Healthy Control Group

Parameter	BD II	Control Group	*P* Value
No. of participants	37	37	
Age (y)	26.37 (8.51)	27.05 (8.65)	.736*
Sex			.813†
No. of men	22	23	
No. of women	15	14	
Years of education	13.98 ± 4.98	15.19 ± 2.91	.104*
Age at onset (y)	21.17 ± 8.83	NA	
Mean no. of episodes	2.51 ± 1.60	NA	
24-item HDRS score (points)	27.86 ± 5.86	NA	
YMRS score (points)	1.45 ± 1.36	NA	
Duration of illness (mo)	43.85 ± 10.66	NA	

Note.—Unless otherwise indicated, data are means ± standard deviation. HDRS = Hamilton Depression Rating Scale, YMRS = Young Mania Rating Scale, NA = not applicable.

* *P* values obtained by independent sample *t* tests.

† *P* value for sex distribution obtained by χ^2 test.

FCS Values

Figure 1 shows the FCS maps of healthy control and BD groups. For the healthy control group, regions with high FCS values were mainly located in the default-mode network (including posterior cingulate cortex and precuneus, medial prefrontal and parietal cortices, and lateral temporal and parietal cortical regions), lateral prefrontal cortex, temporal-parietal junction and visual cortex, and bilateral occipital cortices. Visual inspection indicated that the spatial distributions of FCS in the BD group were similar to those of the healthy control group. However, statistical analysis revealed that, compared with the healthy control participants, the patients with BD showed significantly decreased FCS values in the default-mode network

Figure 1

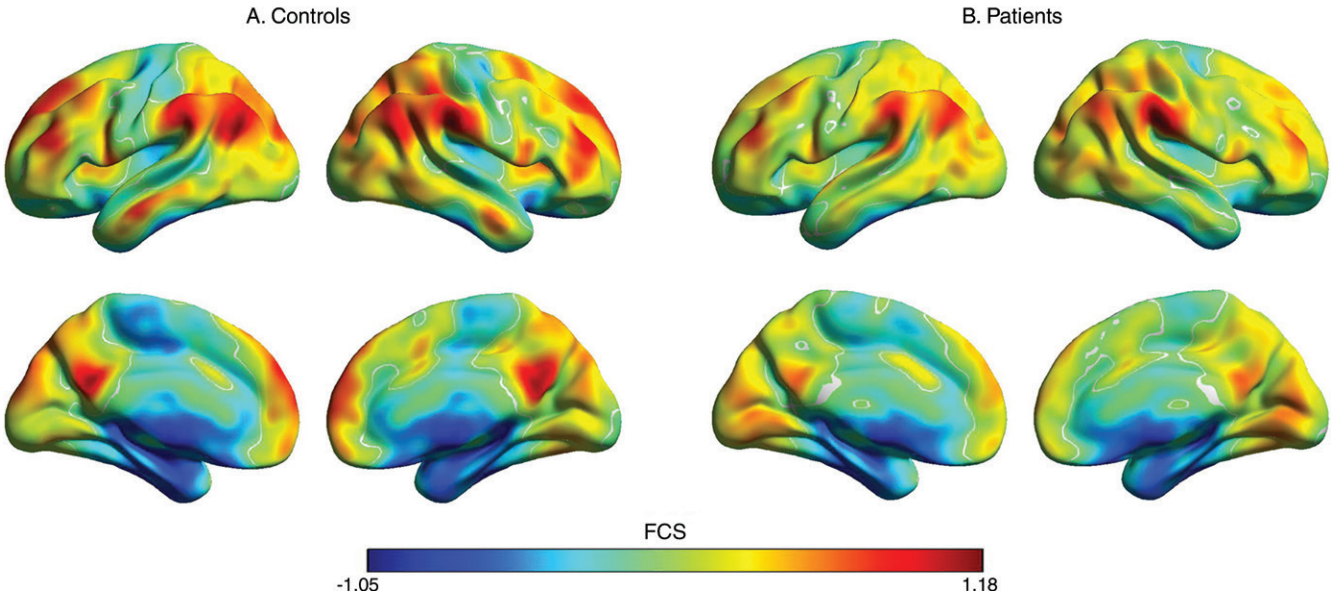

Figure 1: Mean FCS maps within the healthy control group and the BD group.

(ie, bilateral medial prefrontal cortex, bilateral middle temporal gyrus, left precuneus, and right posterior cingulate cortex), right supramarginal gyrus and angular gyrus, right superior frontal gyrus, and right superior parietal gyrus. The patients with BD showed increased FCS values in the bilateral temporal pole (including the parahippocampal gyrus and amygdale), left anterior cingulate cortex, left superior temporal gyrus, right lingual gyrus, and left anterior lobe of the cerebellum ($P < .05$; AlphaSim corrected) (Fig 2, Table 2).

Correlational Analysis

Bonferroni correction was used for the multiple comparisons when Pearson correlation analysis was performed. There were no significant correlations between altered FCS values and any clinical variables in patients with BD.

Discussion

We used resting-state functional MR imaging and voxel-based graph theory analysis to study whole-brain functional connectivity patterns in patients with nonmedicated bipolar II depression and healthy control participants. The primary finding of this study was that patients with BD II showed decreased FCS mainly in the default-mode network, right supramarginal gyrus, right superior frontal gyrus, and right parietal lobe and increased FCS in the limbic structures (ie, parahippocampal gyrus, and amygdale and cingulate gyrus), left superior temporal gyrus, right occipital lobe, and cerebellum.

The default-mode network was implicated in self-referential and reflective activity, including episodic memory retrieval, inner speech, mental images, emotions, and planning future events (28). Previous neuroimaging studies (29) reported that default-mode network abnormalities are associated with multiple mental disorders, such as Alzheimer disease, schizophrenia, depression, and BD, although results were inconsistent. Some evidence (11,29) suggests that abnormalities within the default-mode network may underlie cognitive and affective processing problems in psychiatric conditions. In this study, patients with BD II showed decreased FCS in the default-mode network regions, including the bilateral medial prefrontal cortex, middle temporal gyrus, precuneus, and posterior

Figure 2

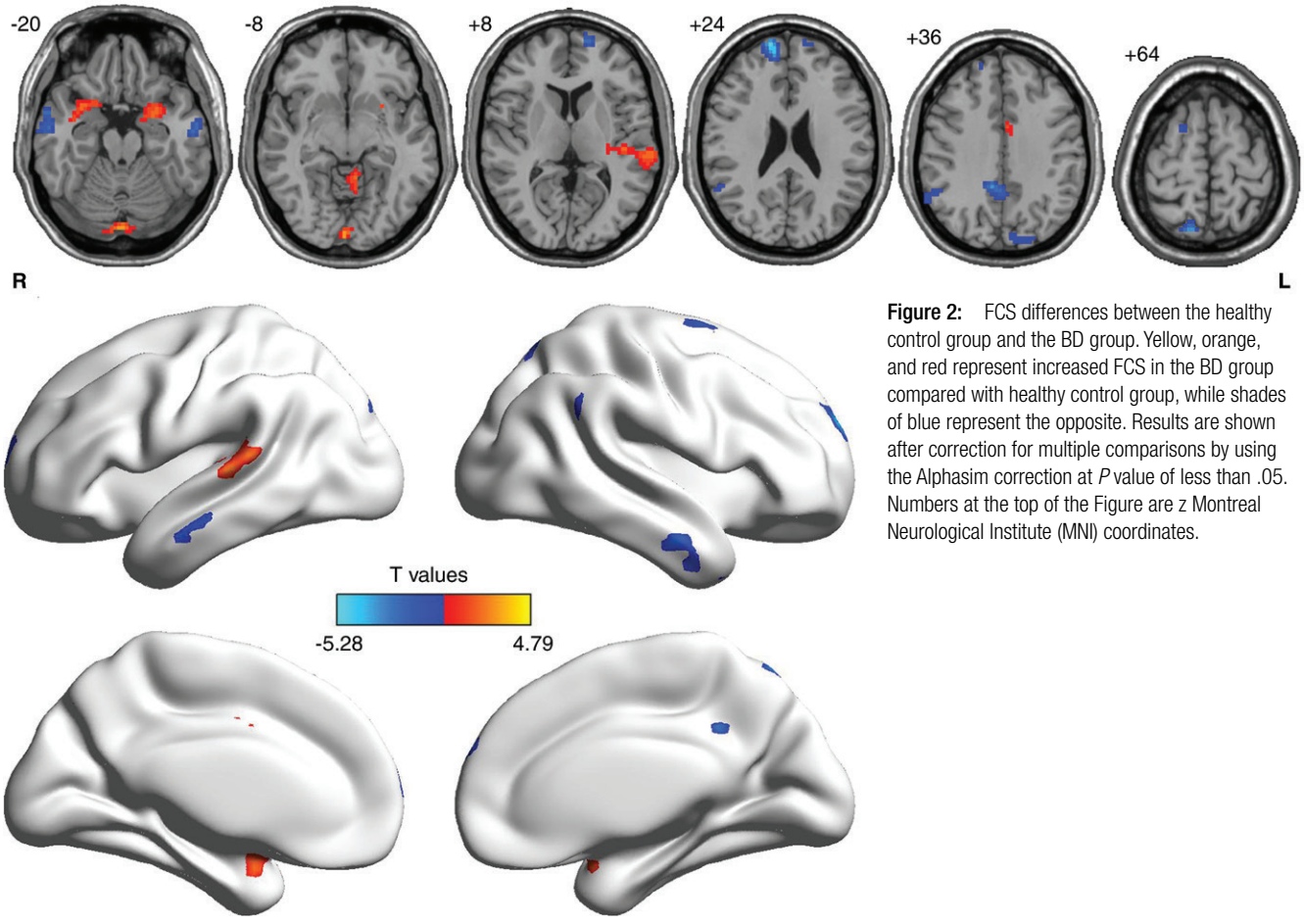

Figure 2: FCS differences between the healthy control group and the BD group. Yellow, orange, and red represent increased FCS in the BD group compared with healthy control group, while shades of blue represent the opposite. Results are shown after correction for multiple comparisons by using the Alphasim correction at *P* value of less than .05. Numbers at the top of the Figure are z Montreal Neurological Institute (MNI) coordinates.

Table 2

Regions that Show FCS Differences between Groups

Brain Regions	Brodmann Area	Montreal Neurologic Institute Coordinates			Peak *t* Value	Cluster Size (voxel)
		x-Axis	y-Axis	z-Axis		
Regions that show decreased FCS in BD patients vs healthy control participants						
Right middle temporal gyrus	21, 20	51	−3	−3	−4.189	163
Left middle temporal gyrus	21	−60	−9	−21	−3.613	51
Right medial prefrontal cortex	10	15	63	27	−5.275	114
Left medial prefrontal cortex	10	−18	66	18	−3.882	62
Right supramarginal gyrus	40	57	−51	30	3.640	51
Left pecuneus	19	−24	−90	33	−3.729	68
Right posterior cingulate cortex	31	9	−45	36	−4.020	49
Right superior parietal lobule	7	15	−69	60	−4.392	53
Right superior frontal gyrus	6	21	0	69	−4.155	45
Regions that show increased FCS in BD patients vs healthy control participants						
Left temporal pole	34, 28	−27	3	−24	3.709	86
Right temporal pole	38, 28	33	6	−24	3.668	55
Left anterior cingulate cortex	24	−6	−6	42	3.599	43
Left superior temporal gyrus	41, 42	−63	−27	6	3.859	170
Right lingual gyrus	18, 17	3	−93	−12	4.509	71
Left cerebellum		−3	−54	−3	4.791	75

Note.—$P < .05$, corrected for multiple comparisons.

cingulate cortex. Several studies that used independent component analysis of resting-state functional MR imaging data reported reduced connectivity within the default-mode network in patients with BD (30–32), which supports our findings of disturbed integrity of the default-mode functional network. Unlike independent component analysis or seed-based approaches, whole-brain FCS mapping measures take into account the relationship of a given region with the entire functional connectome, and not just its relationship to individual regions or to separate larger components (26). A recent study (18) found FCS reduction in the medial prefrontal cortex was correlated with symptomatic improvement in patients with major depressive disorder, which suggested that the medial prefrontal cortex connectivity may act as an objective indicator of the clinical response of depression patients to antidepressant treatment. However, we did not find significant correlations between altered FCS values and any clinical measures in patients with BD (corrected for multiple comparisons). Taken together, these findings tended to suggest an aberrant hub role of default-mode network -related regions in the brain functional network in patients with BD.

The limbic system is the central part of the so-called emotional brain circuitry, dedicated to the processing and regulation of emotion (33,34). Our study revealed altered FCS in the cingulate gyrus, parahippocampa gyrus, and amygdale in BD II, which suggested disrupted functional connectivity in the limbic system. In particular, we found increased FCS in bilateral parahippocampa gyrus and amygdale, and decreased FCS in the frontal lobe in BD. Previous task-based and resting-state functional MR imaging studies reported abnormal frontal-limbic circuit in patients with BD, such as hypoactivation of the frontal lobe (35), hyperactivation of the limbic structures (35,36), and abnormal connectivity between frontal and limbic structures (8,9,37,38). Thus, these studies combined with our results suggest that the mood dysregulation in BD may be explained by the imbalance between the limbic and frontal networks, and the frontal-limbic circuit may be at the root of the pathogenesis of BD.

In addition, we also found increased FCS in cerebellum in patients with BD. Evidence suggests a possible involvement of the cerebellum in cognition, emotion processing, and behavior. The cerebellum has widespread connections with multiple regions of the frontal cortices and limbic regions (38). Several previous studies demonstrated that the cerebellum exhibits abnormalities in functional activation (4,7,39,40) and morphologic structure (39,41,42) in BD. Therefore, our findings provide additional evidence for the involvement of cerebellar dysfunction in the pathophysiologic structure of BD.

Our study has limitations. First, the sample size of this study was relatively small, and results will require

replication in a larger study. Second, although many graph metrics could be used to identify the functional brain networks, we used FCS because it was difficult to calculate other graph metrics due to a highly computational load in a network greater than 60 000 nodes. Third, without a group of patients with BD in a euthymic episode, it is still not clear whether altered FCS is specific to the depression episode of BD or shared by all episodes of the disease. Further studies that use a prospective design may clarify this issue.

In conclusion, our study demonstrated that patients with BD have disrupted intrinsic functional connectivity mainly in the default-mode network and limbic system, which might be associated with the pathophysiologic structure of BD. Future work that combines multimodal neuroimaging data could help to provide further valuable information about this disorder.

Disclosures of Conflicts of Interest: Y.W. disclosed no relevant relationships. **S.Z.** disclosed no relevant relationships. **Y.J.** disclosed no relevant relationships. **Y.S.** disclosed no relevant relationships. **B.W.** disclosed no relevant relationships. **T.L.** disclosed no relevant relationships. **J.P.** disclosed no relevant relationships. **L.H.** disclosed no relevant relationships.

References

1. Merikangas KR, Akiskal HS, Angst J, et al. Lifetime and 12-month prevalence of bipolar spectrum disorder in the National Comorbidity Survey replication. Arch Gen Psychiatry 2007;64(5):543–552.
2. Biswal B, Yetkin FZ, Haughton VM, Hyde JS. Functional connectivity in the motor cortex of resting human brain using echo-planar MRI. Magn Reson Med 1995;34(4):537–541.
3. Liu CH, Li F, Li SF, et al. Abnormal baseline brain activity in bipolar depression: a resting state functional magnetic resonance imaging study. Psychiatry Res 2012;203(2-3):175–179.
4. Liu CH, Ma X, Wu X, et al. Resting-state abnormal baseline brain activity in unipolar and bipolar depression. Neurosci Lett 2012;516(2):202–206.
5. Vargas C, López-Jaramillo C, Vieta E. A systematic literature review of resting state network--functional MRI in bipolar disorder. J Affect Disord 2013;150(3):727–735.
6. Wang X, Xia M, Lai Y, et al. Disrupted resting-state functional connectivity in minimally treated chronic schizophrenia. Schizophr Res 2014;156(2-3):150–156.
7. Liang MJ, Zhou Q, Yang KR, et al. Identify changes of brain regional homogeneity in bipolar disorder and unipolar depression using resting-state FMRI. PLoS One 2013;8(12):e79999.
8. Anand A, Li Y, Wang Y, Lowe MJ, Dzemidzic M. Resting state corticolimbic connectivity abnormalities in unmedicated bipolar disorder and unipolar depression. Psychiatry Res 2009;171(3):189–198.
9. Anticevic A, Brumbaugh MS, Winkler AM, et al. Global prefrontal and fronto-amygdala dysconnectivity in bipolar I disorder with psychosis history. Biol Psychiatry 2013;73(6):565–573.
10. Chai XJ, Whitfield-Gabrieli S, Shinn AK, et al. Abnormal medial prefrontal cortex resting-state connectivity in bipolar disorder and schizophrenia. Neuropsychopharmacology 2011;36(10):2009–2017.
11. Ongür D, Lundy M, Greenhouse I, et al. Default mode network abnormalities in bipolar disorder and schizophrenia. Psychiatry Res 2010;183(1):59–68.
12. Palaniyappan L, Cousins DA. Brain networks: foundations and futures in bipolar disorder. J Ment Health 2010;19(2):157–167.
13. Brier MR, Thomas JB, Fagan AM, et al. Functional connectivity and graph theory in preclinical Alzheimer's disease. Neurobiol Aging 2014;35(4):757–768.
14. Dai Z, Yan C, Li K, et al. Identifying and mapping connectivity patterns of brain network hubs in Alzheimer's disease. Cereb Cortex 2015;25(10):3723–3742.
15. Lei D, Li K, Li L, et al. Disrupted functional brain connectome in patients with posttraumatic stress disorder. Radiology 2015;276(3):818–827.
16. Liu Y, Liang M, Zhou Y, et al. Disrupted small-world networks in schizophrenia. Brain 2008;131(Pt 4):945–961.
17. Gong Q, He Y. Depression, neuroimaging and connectomics: a selective overview. Biol Psychiatry 2015;77(3):223–235.
18. Wang L, Xia M, Li K, et al. The effects of antidepressant treatment on resting-state functional brain networks in patients with major depressive disorder. Hum Brain Mapp 2015;36(2):768–778.
19. Kim DJ, Bolbecker AR, Howell J, et al. Disturbed resting state EEG synchronization in bipolar disorder: A graph-theoretic analysis. Neuroimage Clin 2013;2:414–423.
20. Tomasi D, Volkow ND. Functional connectivity density mapping. Proc Natl Acad Sci U S A 2010;107(21):9885–9890.
21. Wang Y, Zhong S, Jia Y, Zhou Z, Zhou Q, Huang L. Reduced interhemispheric resting-state functional connectivity in unmedicated bipolar II disorder. Acta Psychiatr Scand 2015;132(5):400–407.
22. Chao-Gan Y, Yu-Feng Z. DPARSF: A MATLAB toolbox for "pipeline" data analysis of resting-state fMRI. Front Syst Neurosci 2010;4:13.
23. Wang J, Wang X, Xia M, Liao X, Evans A, He Y. GRETNA: a graph theoretical network analysis toolbox for imaging connectomics. Front Hum Neurosci 2015;9:386.
24. Buckner RL, Sepulcre J, Talukdar T, et al. Cortical hubs revealed by intrinsic functional connectivity: mapping, assessment of stability, and relation to Alzheimer's disease. J Neurosci 2009;29(6):1860–1873.
25. Hou JM, Zhao M, Zhang W, et al. Resting-state functional connectivity abnormalities in patients with obsessive-compulsive disorder and their healthy first-degree relatives. J Psychiatry Neurosci 2014;39(5):304–311.
26. Zuo XN, Ehmke R, Mennes M, et al. Network centrality in the human functional connectome. Cereb Cortex 2012;22(8):1862–1875.
27. Vul E, Pashler H. Voodoo and circularity errors. Neuroimage 2012;62(2):945–948.
28. Greicius MD, Menon V. Default-mode activity during a passive sensory task: uncoupled from deactivation but impacting activation. J Cogn Neurosci 2004;16(9):1484–1492.
29. Broyd SJ, Demanuele C, Debener S, Helps SK, James CJ, Sonuga-Barke EJ. Default-mode brain dysfunction in mental disorders: a systematic review. Neurosci Biobehav Rev 2009;33(3):279–296.
30. Calhoun VD, Maciejewski PK, Pearlson GD, Kiehl KA. Temporal lobe and "default" hemodynamic brain modes discriminate between schizophrenia and bipolar disorder. Hum Brain Mapp 2008;29(11):1265–1275.
31. Khadka S, Meda SA, Stevens MC, et al. Is aberrant functional connectivity a psychosis endophenotype? A resting state functional magnetic resonance imaging study. Biol Psychiatry 2013;74(6):458–466.
32. Meda SA, Ruaño G, Windemuth A, et al. Multivariate analysis reveals genetic associations of the resting default mode network in psychotic bipolar disorder and schizophrenia. Proc Natl Acad Sci U S A 2014;111(19):E2066–E2075.

33. Lotfi E, Akbarzadeh-T MR. Practical emotional neural networks. Neural Netw 2014; 59:61–72.

34. Roxo MR, Franceschini PR, Zubaran C, Kleber FD, Sander JW. The limbic system conception and its historical evolution. ScientificWorldJournal 2011;11:2428–2441.

35. Chen CH, Suckling J, Lennox BR, Ooi C, Bullmore ET. A quantitative meta-analysis of fMRI studies in bipolar disorder. Bipolar Disord 2011;13(1):1–15.

36. Lim CS, Baldessarini RJ, Vieta E, Yucel M, Bora E, Sim K. Longitudinal neuroimaging and neuropsychological changes in bipolar disorder patients: review of the evidence. Neurosci Biobehav Rev 2013;37(3):418–435.

37. Radaelli D, Sferrazza Papa G, Vai B, et al. Fronto-limbic disconnection in bipolar disorder. Eur Psychiatry 2015;30(1):82–88.

38. Reeber SL, Otis TS, Sillitoe RV. New roles for the cerebellum in health and disease. Front Syst Neurosci 2013;7:83.

39. Phillips JR, Hewedi DH, Eissa AM, Moustafa AA. The cerebellum and psychiatric disorders. Front Public Health 2015;3:66.

40. Wang Y, Zhong S, Jia Y, et al. Interhemispheric resting state functional connectivity abnormalities in unipolar depression and bipolar depression. Bipolar Disord 2015;17(5):486–495.

41. Baldaçara L, Nery-Fernandes F, Rocha M, et al. Is cerebellar volume related to bipolar disorder? J Affect Disord 2011;135(1-3):305–309.

42. Redlich R, Almeida JJ, Grotegerd D, et al. Brain morphometric biomarkers distinguishing unipolar and bipolar depression. A voxel-based morphometry-pattern classification approach. JAMA Psychiatry 2014;71(11): 1222–1230.